Journal of Electroanalytical Chemistry 784 (2017) 25–32

Contents lists available at ScienceDirect

Journal of Electroanalytical Chemistry

journal homepage: www.elsevier.com/locate/jelechem

Theoretical model of ion transfer-electron transfer coupled reactions at the thick-film modified electrodes

Franco Martín Zanotto, Ricardo Ariel Fernández , Sergio Alberto Dassie*

Instituto de Investigaciones en Fisicoquímica de Córdoba (INFIQC), CONICET, Departamento de Fisicoquímica, Facultad de Ciencias Químicas, Universidad Nacional de Córdoba, X5000 HUA Ciudad Universitaria, Córdoba, Argentina

ARTICLE INFO

Article history:
Received 28 September 2016
Received in revised form 10 November 2016
Accepted 16 November 2016
Available online 26 November 2016

Keywords:
Electron transfer-ion transfer reactions
Thick-film
Ion distribution
Competitive ion transfer reactions

ABSTRACT

The theory of cyclic voltammetry of ion transfer-electron transfer coupled reactions in a thick organic film modified electrode is developed. The model system consists of a planar electrode completely covered by an organic phase, which in turn is in contact with an aqueous phase, each containing a supporting electrolyte. It is shown that the coupling between the ion transfer-electron transfer processes at both, solid|liquid and liquid|liquid interfaces, has a marked effect on the shape of the voltammogram. The model allows the analysis of the system in different experimental conditions. In particular, the results for different concentration ratios of the redox probe and supporting electrolytes are presented. The variation of the potential of the solid|liquid and the liquid|liquid interfaces reflects changes in concentration of the species involved. This variation is presented as a descriptor of the shape of the voltammograms. The theoretical results are contrasted with experimental behaviour reported in literature.

1. Introduction

The transfer of charged species through a liquid|liquid interface has been studied extensively in recent years [1–9]. These heterogeneous charge transfer can be divided into ion transfer and electron transfer, while ion transfer can be either simple or assisted by a ligand dissolved in the system [5,10,11]

In general, the classic four-electrode system with a single polarized interface [12] has been widely used to study simple ion-transfer reactions, ion-transfer reactions assisted by a ligand or ionophore, and electron transfer-ion transfer (ET-IT) reactions between a hydrophilic and a hydrophobic redox couple [5,9]. In the last years, three-phase electrodes [13–22] and thin film-modified electrodes [20,23-32] emerged as a simple but powerful experimental tool for studying coupled ET-IT reactions [33–37]. In the case of three-phase electrodes, the electrode surface is not covered completely by the organic phase so an interface exists between the three adjacent phases. The electrode reaction starts at the three phase junction and then propagates towards the centre of the organic phase volume, which has no supporting electrolyte. On the other hand, in the case of thin organic-film-modified electrodes, the electrode surface is completely covered by the organic phase. For this reason, the organic phase must contain supporting electrolyte to ensure sufficiently high conductivity to perform electrochemical measurements. The working principle of both electrochemical configurations is based on the electroneutrality of each phase [37,38].

In the course of the electrochemical experiment the electrode reaction of the redox compound (neutral redox-active probe) is coupled with simultaneous charge compensating ion transfer reaction at the other side of the liquid phase. In voltammetric experiments, both the electron and ion transfer processes are recorded together [37]. Theoretical models have provided valuable contributions to thermodynamics, kinetics and ion transfer mechanism across the three-phase electrodes [39–44] and thin film-modified electrodes [45–48].

Recently, a new strategy based on a thick organic film modified electrode was developed and experimentally verified by Niu and coworkers [49]. This strategy is based on an electrode completely covered by an organic phase film of suitable thickness which ensures that the charged product of the redox reaction is kept away from the liquid|liquid interface. This experimental condition can be satisfied at high scan rates in cyclic voltammetry (i.e. greater than 0.1 V s^{-1}), where the electrochemical experiment time is very short. In this experimental condition, the electroneutrality of the organic phase is maintained by the simultaneous injection of ions through the liquid|liquid interface. The authors present a thermodynamic treatment of the coupled electron-ion transfer reactions that allows them to obtain the relationship between the potential of the global process and the concentration of the analyte ion [49].

* Corresponding author.
E-mail address: sdassie@fcq.unc.edu.ar (S. Dassie).

http://dx.doi.org/10.1016/j.jelechem.2016.11.044
1572-6657/

Herein, a model of thick organic film modified electrode that allows analysing the system in different experimental conditions is developed. In particular, the results for different concentration ratios of the redox probe and transferring ion are presented. The variation of the potential of the solid|liquid (S|L) and the liquid|liquid (L|L) interfaces reflects changes in concentration of the species involved. This variation is presented as a descriptor of the shape of the voltammograms. The theoretical results are contrasted with experimental behaviours reported in literature.

2. Theory

The coupled ET-IT process is considered in this model. This follows from the electroneutrality condition in each phase. Electron transfer (ET) is limited to a one electron process, between a solid electrode and an electrically neutral reduced species dissolved in the organic phase. Ion transfer (IT) can occur for any monovalent ion from the electrolytes involved in the electrolytic organic and aqueous phases. Thus, the possible equilibria can be written as:

$$\mathrm{Red}_{(o)} \rightleftharpoons \mathrm{Ox}^{+}_{(o)} + e^{-} \quad \text{(R.1)}$$

$$\mathrm{Anion}^{-}_{(w)} \rightleftharpoons \mathrm{Anion}^{-}_{(o)} \quad \text{(R.2)}$$

$$\mathrm{Cation}^{+}_{(o)} \rightleftharpoons \mathrm{Cation}^{+}_{(w)} \quad \text{(R.3)}$$

The following assumptions for the calculation of the current-potential response are made:

1. The interfaces between the aqueous and the organic phase and between the electrode and organic phase are stationary and planar.
2. Both phases remain quiescent and contain enough inert electrolyte so that mass transport takes place only by diffusion. The potential drop due to solution resistance is neglected.
3. The presence of H^+ and HO^- ions from water autoprotolysis is neglected.
4. The partition of the redox species to the aqueous phase, either electrically charged (Ox^+) or neutral (Red), is neglected. Transfer of the other ions through the interface is reversible and diffusion controlled, dependent on the Nernst equation.
5. The redox reaction taking place at the electrode surface is reversible and diffusion controlled, dependent on the Nernst equation.
6. The thickness of the organic phase is large enough to avoid overlapping between the diffusion fronts of the species generated or consumed on the solid|liquid interface and the liquid|liquid interface.
7. Both interfaces present the same surface area, large enough for edge effects to be negligible. Therefore the semi-infinite linear condition is assumed.
8. Since the electron transfer and ion transfer processes are coupled, the current at both interfaces must be equal.
9. The activity coefficients for all species are assumed to be equal to one.
10. Neither double-layer effects, adsorption nor ion-pair formation are considered in the model.
11. The applied potential is distributed between the S|L interface and the L|L interface at any time. The potential difference on the former defines the concentration ratio of the redox species and on the latter the ion concentration ratios.

The model considers a solid electrode completely covered by a film of organic phase of thickness L containing a redox couple (Red and Ox^+) and an explicit supporting electrolyte, in contact with an aqueous phase containing completely dissociated electrolytes, as shown in Fig. 1 (the model is still valid if the organic and aqueous solutions are interchanged [32], or even for other solvent pairs, such as ionic liquid|aqueous solution and ionic liquid|organic solution interfaces[50]). Similar approaches combining coupled ion transfer-ion transfer were previously described for supported liquid membranes [51–54]

In this work, the following completely dissociated electrolytes are considered: MX, KA and NZ initially dissolved in the aqueous phase (NZ is the explicit supporting electrolyte), and OY, which is the organic explicit supporting electrolyte. In order to obtain the concentrations as a function of distance to the electrode and time, Fick's laws of diffusion were solved using explicit finite difference [55–60].

The determination of the initial equilibrium state involves the calculation of the distribution potential ($\Delta^{w}_{o}\phi_{eq}$) for this system, which in turn depends on the standard transfer potential of each ion i ($\Delta^{w}_{o}\phi^{\circ}_{i}$) and the initial concentration of ions in each phase, obtained by solving Eq. (8) from Ref. [38]:

$$\sum_i z_i \frac{c_i^{w} + r c_i^{o}}{1 + r(\theta_{eq}\theta_i)^{z_i}} = 0 \quad (1)$$

where z_i is the charge of ion i (in this model $z_i = +1$ or $z_i = -1$), $\theta_{eq} = \exp(\frac{F}{RT}\Delta^{w}_{o}\phi_{eq})$ and $\theta_i = \exp(-\frac{F}{RT}\Delta^{w}_{o}\phi^{\circ}_{i})$. c_i^{w} and c_i^{o} are the equilibrium concentrations of the ion i in the aqueous and organic phases respectively, r is the volume ratio between the organic and aqueous phase. More details on the solution of this equation are presented in the appendix.

The initial applied potential difference ($t = 0$) was set in all cases as the sum of the potential difference at each interface: $E(0) = \Delta^{s}_{o}\phi(0) + [-\Delta^{w}_{o}\phi(0)]$. The Galvani potential difference between the electrode and the organic phase ($\Delta^{s}_{o}\phi(0)$) is calculated from the initial

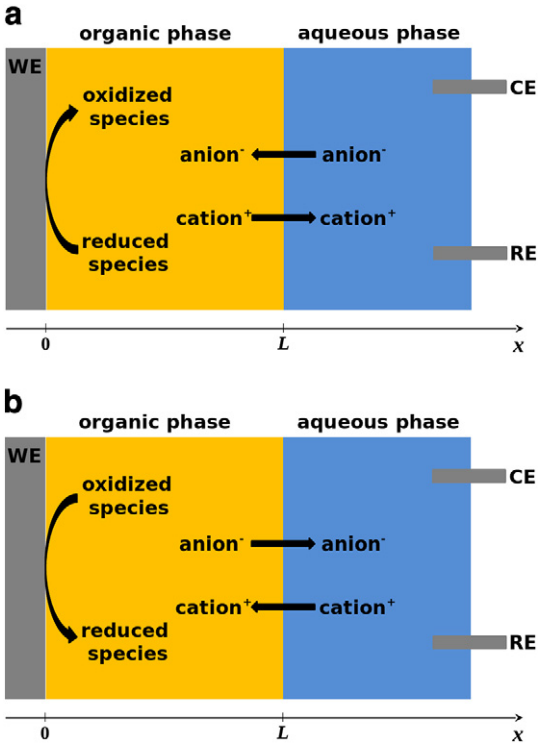

Fig. 1. Scheme of the electrochemical cell considered in the model showing coupled electron transfer and ion transfer processes resulting in positive current (top) and negative current (bottom). WE: working electrode. CE: counter electrode. RE: reference electrode.

concentrations of Ox^+ and Red. $\Delta_o^w\phi(0)$ is the distribution potential at the L|L interface.

When reaction (R.1) is coupled to either Eq. (R.2) or (R.3), the following Nernst equation can be written for any ion i as a boundary condition [61]:

$$\frac{c_{Ox^+}(0,t)}{c_{Red}(0,t)}\left[\frac{c_i^w(L,t)}{c_i^o(L,t)}\right]^{z_i} = \exp\left\{\frac{F}{RT}\left[E(t) - \Delta_o^s\phi_{Red}^\circ + \Delta_o^w\phi_i^\circ\right]\right\} \quad (2)$$

where $c_{Ox^+}(0,t)$, and $c_{Red}(0,t)$ are the redox species concentrations at the S|L interface ($x = 0$) at any time, $c_i^w(L,t)$ and $c_i^o(L,t)$ are the ionic species concentrations at the L|L interface ($x = L$) at any time (see Fig. 1). $\Delta_o^s\phi_{Red}^\circ$ is the standard potential associated to reaction (R.1). This condition assures that for each interface, its individual Nernst equation (for ET or IT reactions) will be satisfied. Each presents its own potential difference, so that $E(t) = \Delta_o^s\phi(t) - \Delta_o^w\phi(t)$ at each time [45].

With the value of $\Delta_o^w\phi(0)$ and also initial ion distribution at the L|L interface, by fixing the ratio $\frac{c_{Ox^+}(x,0)}{c_{Red}(x,0)}$ it is possible to obtain $\Delta_o^s\phi(0)$ and define an initial external potential difference $E(0)$ from Eq. (2).

The initial concentration of Red species was left as a variable. For values of $\frac{c_{Ox^+}(x,0)}{c_{Red}(x,0)}$ lower than 10^{-4}, the voltammogram remains unaltered. This ratio was fixed at 10^{-6} unless otherwise mentioned.

At $x = 0$ or $x = L$, the following boundary conditions must be met for the redox species and every ion i:

$$D_{Ox^+}\frac{\partial c_{Ox^+}(0,t)}{\partial x} = -D_{Red}\frac{\partial c_{Red}(0,t)}{\partial x} \quad (3)$$

$$D_i^o\frac{\partial c_i^o(L,t)}{\partial x} = D_i^w\frac{\partial c_i^w(L,t)}{\partial x} \quad (4)$$

where D_{Ox^+} and D_{Red} are the redox species diffusion coefficients at the organic phase and D_i^o and D_i^w are the ionic species diffusion coefficients at the organic and aqueous phase respectively. The coupled ET-IT reactions require the current at both interfaces to be equal. Since their surface areas are the same, this can be expressed by the following equation:

$$\sum_i\left(z_iD_i^w\frac{\partial c_i^w(L,t)}{\partial x}\right) = D_{Ox^+}\frac{\partial c_{Ox^+}(0,t)}{\partial x} \quad (5)$$

Finally, semi-infinite diffusion conditions imply:

$$c_{Ox^+}(L,t) = c_{Ox^+}^{init} \quad (6)$$

$$c_{Red}(L,t) = c_{Red}^{init} \quad (7)$$

$$c_i^w(\infty,t) = c_i^w(x,0) \quad (8)$$

$$c_i^o(0,t) = c_i^o(x,0) \quad (9)$$

for any ion i, where the superindex init denotes initial values for the variable.

A modification of the Powell hybrid method [62–64] was used to solve the equations describing boundary conditions (Eqs. (2) to (9)). Results were checked for step size independence.

Cyclic voltammograms were simulated by varying the total potential as follows:

$$E(t) = \begin{cases} \Delta_o^s\phi(t) - \Delta_o^w\phi(t) + vt & \text{if } t \le \lambda \\ \Delta_o^s\phi(t) - \Delta_o^w\phi(t) + v(2\lambda - t) & \text{if } t > \lambda \end{cases} \quad (10)$$

for a constant potential sweep rate v.

3. Results and discussion

The results are presented in subsections according to the developed model. Four aspects are discussed: the effect of the initial concentrations of the ions and of Red species, the effect of the standard transfer potential of the anion, the case where two ions are available for IT and finally some considerations of experimental interest.

NZ and OY are the aqueous and organic supporting electrolyte, respectively. Consequently, the standard potential of their ions was set to represent typical hydrophobic and hydrophilic ions: $\Delta_O^W\phi_{O^+}^\circ = -0.699$ V, $\Delta_O^W\phi_{Y^-}^\circ = 0.725$ V, $\Delta_O^W\phi_{N^+}^\circ = 0.606$ V, $\Delta_O^W\phi_{Z^-}^\circ = -0.650$ V. These values correspond to Bis(triphenylphosphoranylidene)ammonium, tetrakis(pentafluorophenyl)borate, Na^+ and HO^- ions respectively, across the water|1, 2-dichloroethane interface [49,65-67], just as an example. $c_{NZ,w}^{init}$ was set so that total electrolyte concentration in the aqueous phase was at least 1.0 M, and $c_{OY,o}^{init}$ was fixed at 1.0 M for all simulations. It is expected that as this concentration increases, the possibility of interference also increases. Accordingly, this high concentration is set as an upper bound. Typical concentration values (i.e. around 0.01 M) are expected to present even less interference for the cases shown here.

Diffusion coefficients were set equal to 1.0×10^{-5} cm^2 s^{-1} for all species in both phases.

Unless otherwise mentioned, the rest of the simulation parameters were set as follows: $T = 298.15$ K, $v = 0.500$ V s^{-1}, $\Delta_O^W\phi_{K+}^\circ = 0.400$ V, $\Delta_O^W\phi_{A^-}^\circ = 0.200$ V, $\Delta_O^W\phi_{M^+}^\circ = 0.600$ V, $\Delta_O^W\phi_{X^-}^\circ = -0.300$ V.

All potentials are plotted in reference to $\Delta_o^s\phi_{Red}^\circ$

3.1. Effect of $c_{MX,w}^{init}/c_{Red}^{init}$

In this section the transfer of X^- coupled with the oxidation of Red species is analysed as a function of the ratio of initial concentrations of MX in the aqueous phase and the redox species. The shape of the current-potential profiles for ET-IT processes depend on this ratio, thus the peak-to-peak potential difference (ΔE_{peak}) is a useful simple indicator that gives information about the evolution of the potential difference on each of the interfaces on which the coupled processes occur. It is also important to remark that this ratio is a reduced parameter, as long as the presence of other electrolytes does not interfere with the measurement.

Fig. 2a presents ΔE_{peak} as a function of $\log\left(\frac{c_{MX,w}^{init}}{c_{Red}^{init}}\right)$ for the ET-IT processes involving X^-. The dotted vertical line represents the maximum ratio experimentally attainable in an electrochemical cell, considering a maximum solubility of 0.1 M for Red species and a detection limit of 1×10^{-5} M for the species that controls the current. It can be seen that although both ET and IT are reversible processes, the coupling between them changes the shape of the voltammograms. This behaviour correlates with the evolution in mid-peak potential, $E_{mid}\left(= \frac{1}{2}\left(E_{peak}^{forward\ scan} + E_{peak}^{reverse\ scan}\right)\right)$, shown in Fig. 2b. Both reach a maximum for $\log\left(\frac{c_{MX,w}^{init}}{c_{Red}^{init}}\right) = 0.0$. When $c_{MX,w}^{init} > c_{Red}^{init}$, the Red species limits the global process, so that E_{mid} decreases 59 mV per decade of concentration ratio change. In addition, when $c_{MX,w}^{init} \gg c_{Red}^{init}$, the plot of E_{mid} reaches a constant value and ΔE_{peak} is close to 59 mV. This behaviour arises because for high initial concentration of MX, $c_{M^+}^o(x,0)$ (in the organic phase) stops being negligible and the transfer of M^+ from the organic to the aqueous phase is significant, this results in a current response that is independent of $c_{MX,w}^{init}$.

The same effect is observed when the initial conditions are set so that the same ion is present in significant concentration in both phases (e.g. when electrolytes sharing a common cation or anion are dissolved in each phase). In these cases, the L|L interface becomes non-polarizable [68,69]. Thus, the applied potential only affects

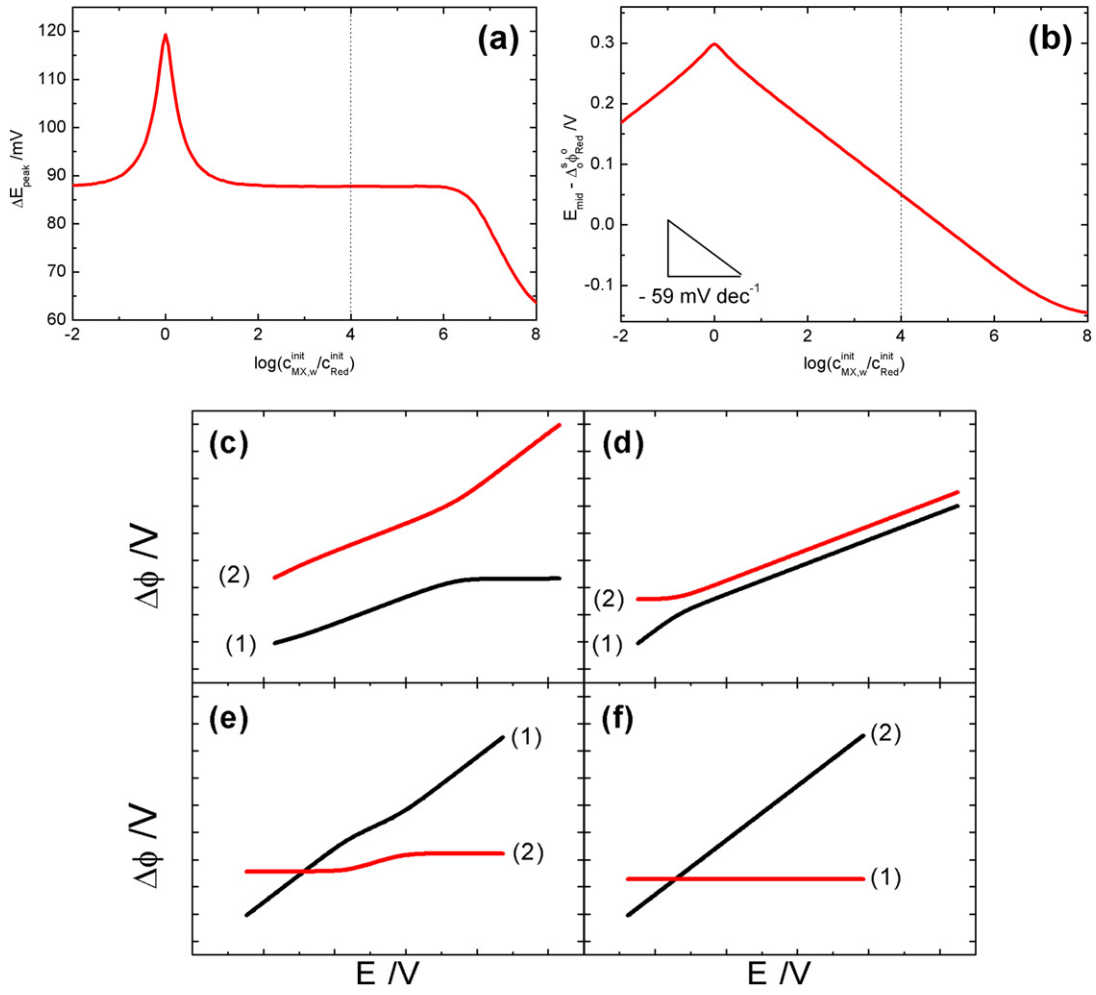

Fig. 2. (a) Peak-to-peak potential difference and (b) mid-peak potential as a function of $\log\left(\frac{c^{init}_{MX,w}}{c^{init}_{Red}}\right)$ in voltammograms obtained for ET coupled with IT of X^- from aqueous to organic phase, with explicit supporting electrolyte in both phases. (c)–(f) Potential difference at each interface as a function of external applied potential: $\Delta^s_o\phi$ (1) and $-\Delta^w_o\phi$ (2) corresponding to $\log\left(\frac{c^{init}_{MX,w}}{c^{init}_{Red}}\right) = -2$ (c), 0 (d), 3 (e) and 8 (f)

the S|L interface and a classic response for a reversible process is obtained (not shown here). This emphasizes the importance of taking into account the equilibrium ion distribution in this model.

The deviation from the usual behaviour of a reversible diffusion-controlled electrochemical process can be explained by the evolution in the potential difference at the S|L and L|L interfaces with total potential applied [53,54]. As it has been mentioned before, the sum of the $\Delta\phi$ at both interfaces must be equal to the total external applied potential. In turn, it follows from Eq. (2) that each of these potential differences can be described by their respective Nernst equation. Fig. 2c to f show their value as a function of the total applied potential for different concentration ratios. The sum of these curves must be a linear plot with a slope equal to unity. This can be as a consequence of only one interface changing its potential and the other remaining constant or both interfaces changing their potential at the same time.

For low concentration ratios (i.e. $c^{init}_{MX,w} < c^{init}_{Red}$, Fig. 2c), it can be seen that the perturbation affects both interfaces equally at lower potentials, but affects only the L|L interface at higher potentials, producing a voltammogram with a ΔE_{peak} of around 90 mV. When $\log\left(\frac{c^{init}_{MX,w}}{c^{init}_{Red}}\right) = 0.0$ (Fig. 2d) this perturbation affects in equal measure both interfaces and for this special case a maximum ΔE_{peak} of around 120 mV is obtained. When MX is in slight excess (Fig. 2e), it affects mostly the S|L interface, except around the peak potential. This again gives rise to a ΔE_{peak} of 90 mV. Finally, for a great excess of MX (Fig. 2f), the L|L interface cannot be polarized due to substantial partition of aqueous ions to the organic phase, resulting in a classic reversible response with $\Delta E_{peak} = 59$ mV, due to the common-ion effect [68].

It is important to note that a ΔE_{peak} of 90 mV is present for a great set of the experimentally accessible systems. The results presented by Niu and co-workers [49], for which $\log\left(\frac{c^{init}_{MX,w}}{c^{init}_{Red}}\right) \approx 3$, show a peak separation of around 90 mV in every case. Considering that all the systems analysed in this work are electrochemically reversible and the transfer of charged species is a diffusion-controlled process, E_{mid} can be regarded as the half-wave potential ($E_{1/2}$) [70]. Additionally, the same study demonstrates that for this concentration ratio, $E_{1/2,X^-}$ depends linearly on $\log(c^{init}_{MX,w})$, with a slope of −59 mV per decade, which is also in agreement with this model, as can be seen in Fig. 2b. However, care must be taken when concentrations are markedly different, since these observations are only valid for a certain range of concentration ratios. This is especially important in two cases (Fig. 2a and b): a) when the redox species is in excess, since the E_{mid} increases

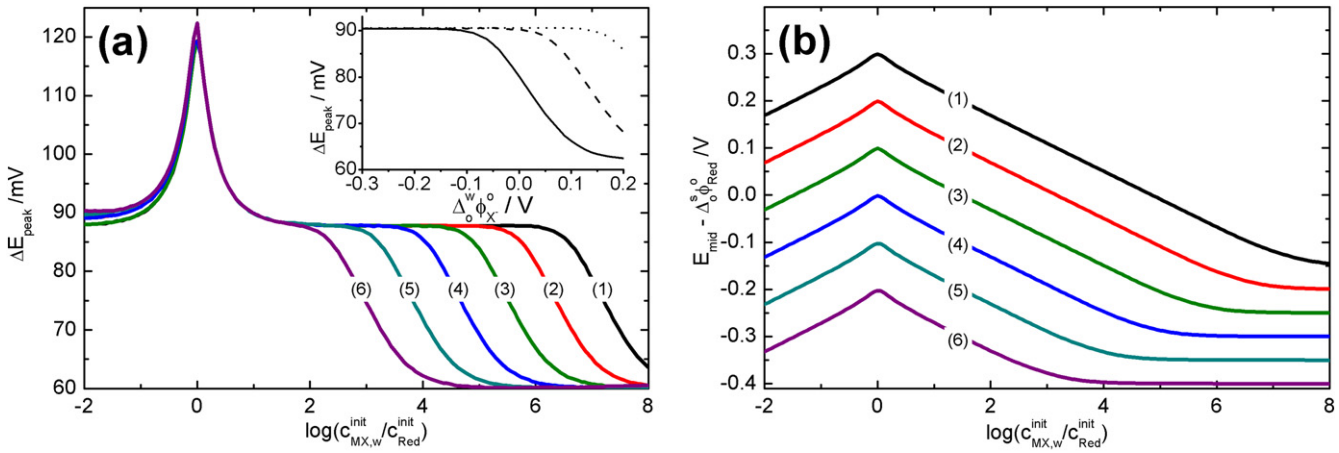

Fig. 3. (a) Peak-to-peak potential difference and (b) mid-peak potential as a function of $\log\left(\frac{c^{init}_{MX,w}}{c^{init}_{Red}}\right)$ in voltammograms obtained for ET coupled with IT of X^- from water to organic phase, with explicit supporting electrolyte on both phases. The curves correspond to different values of $\Delta^W_O\phi^\circ_{X^-} = -0.30$ V (1), −0.20 V (2), −0.10 V (3), 0.00 V (4), 0.10 V (5) and 0.20 V (6). Inset in (a): peak-to-peak potential difference as a function of $\Delta^W_O\phi^\circ_{X^-}$ for three different values of $\log\left(\frac{c^{init}_{MX,w}}{c^{init}_{Red}}\right) = 2.0$ (dotted line), 3.0 (dashed line) and 4.0 (solid line).

with the concentration ratio instead of decreasing. b) When both concentrations are equal or very similar, since ΔE_{peak} is larger, even for reversible ET and IT processes.

3.2. Effect of the standard transfer potential of X^-

The relative hydrophobicity of the anion present in the aqueous phase also influences the coupled processes, hence, another variable of interest is $\Delta^W_O\phi^\circ_{X^-}$. As can be seen in Fig. 3a, for concentration ratios of less than 10^2, $\Delta^W_O\phi^\circ_{X^-}$ has no effect on the shape of the voltammogram, however, for large excess of MX, $\Delta^W_O\phi^\circ_{X^-}$ also influences ΔE_{peak}. As explained in the previous section, for these situations the equilibrium ion distribution, directly related to $\Delta^W_O\phi^\circ_{X^-}$, affects the voltammogram shape. For example, for $\log\left(\frac{c^{init}_{MX,w}}{c^{init}_{Red}}\right) = 4.0$, ΔE_{peak} varies from around 60 mV for $\Delta^W_O\phi^\circ_{X^-} = 0.2$ V to 90 mV for $\Delta^W_O\phi^\circ_{X^-} = -0.1$ V (inset in Fig. 3a).

Fig. 3b also shows that $\Delta^W_O\phi^\circ_{X^-}$ directly modulates the potential at which the process occurs. This indicates that this technique allows for the determination of standard transfer potentials, if a well-known reference ion can be used, as demonstrated by experimental measurements [49].

It should be noted that conditions for which $\Delta E_{peak} < 90$ mV are easily attainable in experiments for semi-hydrophobic anions. In such cases the peak potential cannot be described by a simple dependence on $\Delta^W_O\phi^\circ_{X^-}$. Consequently, care must be taken when voltammograms present $\Delta E_{peak} < 90$ mV.

3.3. Successive ion transfers

When the ion to be transferred (X^-) is in excess with respect to the redox probe, only one process is observed in the voltammogram (corresponding to its transfer to the organic phase coupled with the oxidation of Red species), even in the presence of other ions that could act as interferents. Once the concentration of Red species near the interface is depleted, no more is available to allow the transfer of other ions. In contrast, when the Red species is in excess, the ET reaction can be coupled with several IT processes corresponding to different ions, since a sufficient amount of redox species remains unreacted after every ion is depleted at the L|L interface.

This situation is of experimental interest when one of the ions, for example A^-, is the reference mentioned in Section 3.2, to be used as an internal standard. Fig. 4 shows the voltammograms obtained for different values of $\Delta^W_O\phi^\circ_{X^-}$ and $\Delta^W_O\phi^\circ_{A^-} = -0.2$ V.

For different experiments, when X^- or A^- are added independently in the electrochemical cell, the difference between the peak potential of the two processes is equal to $|\Delta^W_O\phi^\circ_{A^-} - \Delta^W_O\phi^\circ_{X^-}|$, thus the use of ^-A as a reference is straightforward. Remarkably, this is not the case for voltammograms obtained in presence of both ions. For the cases shown in Fig. 4, the peaks potential difference is around 15 mV larger and this discrepancy does not depend on $\Delta^W_O\phi^\circ_{X^-}$. The second process is shifted to positive potentials compared to a voltammogram without X^-. As can be seen in Fig. 5, the potential shift of the second peak depends on the concentration of the species corresponding to the first. This effect is due to the accumulation of a small amount of Ox^+ species at the interface, for example, in the cases shown in Fig. 4, $c^{init}_{Red} = 100$ mM and $c^{init}_{MX,w} = 1.0$ mM, after the first process, $c_{Red}(0,t)$ (at the S|L interface) is reduced to 99 mM and c_{Ox^+} is 1.0 mM. This shifts $\Delta^s_o\phi$ just before the second process occurs, and consequently shifts $\Delta^W_o\phi$.

In order to verify this explanation, voltammograms (1) and (2) are compared in Fig. 6. (1) is in presence of both electrolytes, while (2) is in presence only of KA but with different initial concentration of

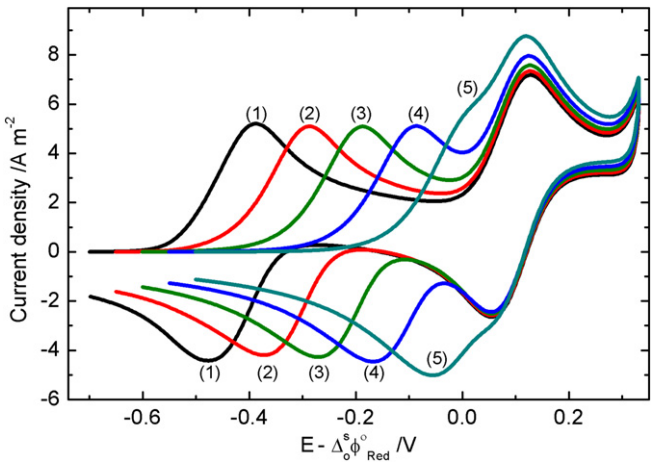

Fig. 4. Voltammograms for the ET reaction coupled with X^- and A^- transfer in excess of Red species for the following conditions: $c^{init}_{Red} = 0.1$ M, $c^{init}_{MX,w} = 1.0$ mM, $c^{init}_{KA,w} = 1.0$ mM, $\Delta^W_O\phi^\circ_{A^-} = -0.20$ V. The curves correspond to $\Delta^W_O\phi^\circ_{X^-} = 0.30$ V (1), 0.20 V (2), 0.10 V (3), 0.00 V (4) and −0.10 V (5).

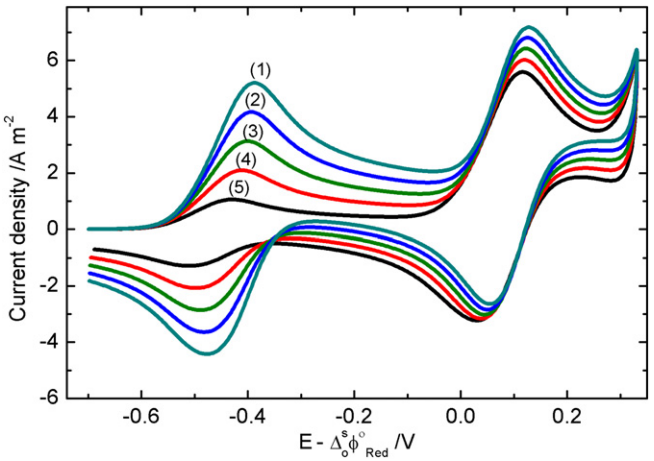

Fig. 5. Voltammograms for the ET reaction coupled with X^- and A^- transfer in excess of Red species for the following conditions: $c^{init}_{Red} = 0.1$ M, $c^{init}_{KA,w} = 1.0$ mM, $\Delta^W_O\phi^\circ_{X^-} = 0.30$ V and $\Delta^W_O\phi^\circ_{A^-} = -0.20$ V. The curves correspond to $c^{init}_{MX,w} = 1.0$ mM (1), 0.8 mM (2), 0.6 mM (3), 0.4 mM (4) and 0.2 mM (5).

the redox species: $c^{init}_{Red} = 99$ mM and $c^{init}_{Ox^+} = 1.0$ mM. For both, the anodic and cathodic peak corresponding to the transfer of A^- occur at the same potentials, 17 mV more positive than that of only KA with the usual concentrations of the redox pair (voltammogram (3)). This confirms that the peak shift is induced by the formation of Ox^+ at the expense of the reduced species. This dependence emphasizes the need for the initial concentration ratio between Ox^+ and Red species to be as low as possible during experiments, since undesired side reactions could produce Ox^+ species and modify the mid-peak potential.

3.4. Application: avoiding interference from the supporting electrolyte

The presence of the organic supporting electrolyte can be a limiting factor for the determination of standard transfer potentials. In the case of hydrophilic anions (e.g. X^-), the transfer of O^+ cation from the organic supporting electrolyte can overlap with the transfer of X^-, yielding difficult to interpret results. This overlap can be quantified by a magnitude defined as the transferred charge across the

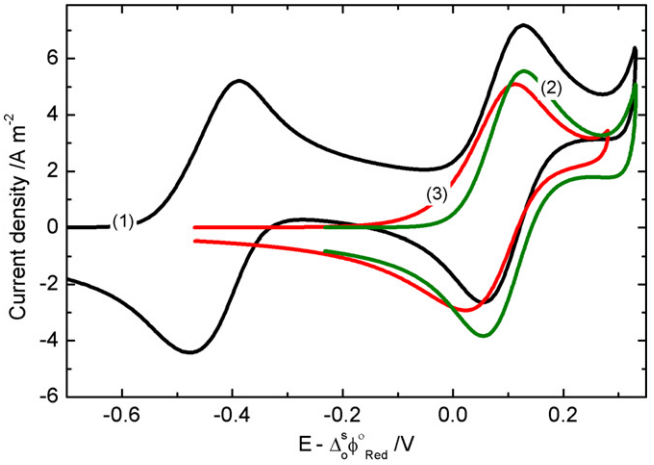

Fig. 6. Voltammograms obtained for the following initial conditions: (1) $c^{init}_{Red} = 100$ mM, $c^{init}_{Ox^+} = 1.0 \times 10^{-4}$ mM, $c^{init}_{KA,w} = 1.0$ mM, $c^{init}_{MX,w} = 1.0$ mM (2) $c^{init}_{Red} = 99$ mM, $c^{init}_{Ox^+} = 1.0$ mM, $c^{init}_{KA,w} = 0.0$ mM, $c^{init}_{MX,w} = 1.0$ mM (3) $c^{init}_{Red} = 100$ mM, $c^{init}_{Ox^+} = 1.0 \times 10^{-4}$ mM, $c^{init}_{KA,w} = 0.0$ mM, $c^{init}_{MX,w} = 1.0$ mM

L|L interface corresponding to the X^- ion divided by the total transferred charge (q_{X^-}/q_{tot}). Undoubtedly, the degree of overlap will be dependent on the difference of half-wave potentials for the two ET-IT processes, which in turn depend on the standard transfer potential of each ion and its initial concentration. Fig. 7a shows q_{X^-}/q_{tot} as a function of $\log(c^{init}_{MX,w}/1.0M)$ for different values of $\Delta^W_O\phi^\circ_{X^-}$. When $q_{X^-}/q_{tot} \geq 0.90$ the error in the determination of $\Delta^W_O\phi^\circ_{X^-}$ is less than 1 mV, accordingly, 0.90 is arbitrarily set as an acceptable ratio. In the cases shown in Fig. 7a, there is a minimum value of $c^{init}_{MX,w}$ for which this condition is met. This minimum value depends on $\Delta^W_O\phi^\circ_{X^-}$. It is noteworthy that it is possible to determine $\Delta^W_O\phi^\circ_{X^-}$ even if it is more negative than $\Delta^W_O\phi^\circ_{O^+}(-0.699\ V)$, as long as the concentrations are adequate.

Niu and co-workers [49] have derived an expression for $E_{1/2,X^-}$, valid when $c^{init}_{MX,w} \gg c^{init}_{Red}$, from which a similar one can be obtained for $E_{1/2,O^+}$:

$$E_{1/2,X^-} = \Delta^o_s\phi^\circ_{Red} - \Delta^o_w\phi^\circ_{X^-} + \frac{RT}{F}\ln\left[\frac{(D^o_{Red})^{1/2}c^{init}_{Red}}{2(D^o_{X^-})^{1/2}c^{init}_{MX,w}}\right] \quad (11)$$

$$E_{1/2,O^+} = \Delta^o_s\phi^\circ_{Red} - \Delta^o_w\phi^\circ_{O^+} + \frac{RT}{F}\ln\left[\frac{(D^o_{Red})^{1/2}c^{init}_{Red}}{2\left(D^o_{O^+}\right)^{1/2}c^{init}_{OY,o}}\right] \quad (12)$$

By subtracting and rearranging the previous equations, the difference in half-wave potentials can be written as:

$$E_{1/2,O^+} - E_{1/2,X^-} = \Delta^o_w\phi^\circ_{X^-} - \Delta^o_w\phi^\circ_{O^+} + \frac{RT}{F}\ln\left(\frac{c^{init}_{MX,w}}{c^{init}_{OY,o}}\right) \quad (13)$$

When the Red species is in defect with respect to MX and OY, q_{X^-}/q_{tot} is only a function of this half-wave potential difference. In other words, $E_{1/2,O^+} - E_{1/2,X^-}$ is a reduced parameter that includes four others: $\Delta^W_O\phi^\circ_{X^-}$, $\Delta^W_O\phi^\circ_{O^+}$, $c^{init}_{MX,w}$ and $c^{init}_{OY,o}$. Fig. 7b shows the curves presented in Fig. 7a as a function of $E_{1/2,O^+} - E_{1/2,X^-}$. All of the curves are superimposed and centred at $\log(c^{init}_{MX,w}/1M) = 0$ when plotted against this parameter. It is clear from this figure that q_{X^-}/q_{tot} is greater than 0.90 when the difference of half-wave potentials is greater than 59 mV.

In light of this theoretical insight, some guidelines can be taken into account to experimentally discern if the organic supporting electrolyte is affecting the determination: firstly, obtain a voltammogram for which the current peak can be doubtlessly assigned to the transfer of O^+ (i.e. very hydrophilic aqueous supporting electrolyte in relatively low concentration). Secondly, obtain a voltammogram for the same initial concentration of OY in presence of X^-. If the difference in E_{mid} is found to be larger than 59 mV, the current peak can be safely assigned to the electron transfer process coupled with X^- transfer. If this is not the case, a lower concentration of OY or a higher concentration of MX can be used and the process repeated.

4. Conclusion

A model for the coupled reversible electron transfer-ion transfer reactions in the thick film configuration was developed. This model takes into account the oxidation of a species in the organic phase and the transfer of an anion from the aqueous to the organic phase (or a cation in the opposite sense). The importance of initial ion distribution at the liquid|liquid interface is stressed.

The shape of the voltammograms obtained depend on the initial concentration ratio between the redox species and the ion involved in the process. This dependence can be explained in terms of the

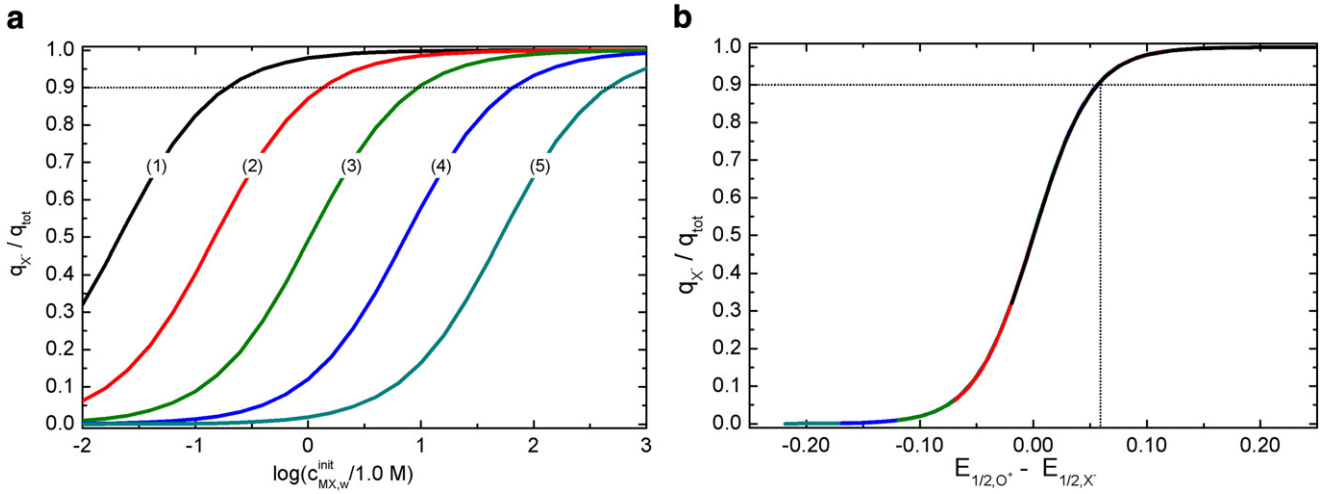

Fig. 7. (a) q_{X^-}/q_{tot} as a function of $\log(c^{init}_{MX,w}/1\ M)$ for $c^{init}_{OY} = 0.01$ M, $c^{init}_{Red} = 1.0 \times 10^{-6}$ M and different values of $\Delta^W_O\phi^\circ_{X^-}$: −0.60 V (1), −0.65 V (2), −0.70 V (3), −0.75 V (4) and −0.80 V (5). (b) q_{X^-}/q_{tot} as a function of $E_{1/2,0^+} - E_{1/2,X^-}$ for the same conditions. Curves (1)–(5) are superimposed. The dotted horizontal line in both plots represent $q_{X^-}/q_{tot} = 0.90$

way in which the external applied potential difference is distributed between the solid|liquid and liquid|liquid interfaces.

The dependence of the mid-peak potential on initial concentration ratio and standard transfer potential of the ion was analysed and a good agreement with reported experimental results was found. This potential is also dependent on whether an ion has been transferred before in the same experiment. Finally, some considerations of experimental interest that allow for minimization of interference by the supporting electrolyte are discussed.

We consider that this model allows for a better understanding of thick-film modified electrodes. An extension of this model could be used to understand other recent experiments with promising applications in energy storage. The ET-IT processes have recently been applied by Girault and coworkers [71] to the development of ion transfer batteries that exploit the Galvani potential difference between aqueous and organic phases.

Acknowledgments

R.A.F. and S.A.D. are Researchers from Consejo Nacional de Investigaciones Científicas y Tecnológicas (CONICET). F.M.Z. thanks CONICET for the fellowship granted. Financial support from CONICET (PIP 00174), Secretaría de Ciencia y Tecnología de la Universidad Nacional de Córdoba (SECyT-UNC) 307-201501-01136-CB and Fondo para la Investigación Científica y Tecnológica (FONCyT) PICT-2012-1820 are gratefully acknowledged.

Appendix

The initial ion distribution for the simulation is calculated from initial concentrations of the electrolytes in their respective phase [38,68,69,72]. Mass balance is considered for each species:

$$c^{init}_{NZ,w} = c^w_{N^+}(x,0) + rc^o_{N^+}(x,0) \tag{14}$$

$$c^{init}_{NZ,w} = c^w_{Z^-}(x,0) + rc^o_{Z^-}(x,0) \tag{15}$$

$$c^{init}_{KA,w} = c^w_{K^+}(x,0) + rc^o_{K^+}(x,0) \tag{16}$$

$$c^{init}_{KA,w} = c^w_{A^-}(x,0) + rc^o_{A^-}(x,0) \tag{17}$$

$$c^{init}_{MX,w} = c^w_{M^+}(x,0) + rc^o_{M^+}(x,0) \tag{18}$$

$$c^{init}_{MX,w} = c^w_{X^-}(x,0) + rc^o_{X^-}(x,0) \tag{19}$$

$$rc^{init}_{OY,o} = c^w_{O^+}(x,0) + rc^o_{O^+}(x,0) \tag{20}$$

$$rc^{init}_{OY,o} = c^w_{Y^-}(x,0) + rc^o_{Y^-}(x,0) \tag{21}$$

with r being the volume ratio, $\frac{V_o}{V_w}$, which in this work was set $r = 1.0$ in every case for simplicity, after performing simulations under different conditions that showed that results for values as low as 0.003 (corresponding to a film of 30 μL immersed in a 10 mL aqueous solution) presented no dependence on r.

The Nernst equation must also be satisfied for each ion at equilibrium potential:

$$\frac{c^o_i(x,0)}{c^w_i(x,0)} = \exp\left[\frac{z_iF}{RT}\left(\Delta^W_o\phi_{eq} - \Delta^W_o\phi^\circ_i\right)\right] \tag{22}$$

where z_i is the charge of ion i.

Lastly, electroneutrality of one of the phases (in this case the aqueous phase) must be considered:

$$\begin{aligned} &c^w_N(x,0) + c^w_K(x,0) + c^w_M(x,0) + c^w_O(x,0) \\ &= c^w_Z(x,0) + c^w_A(x,0) + c^w_X(x,0) + c^w_Y(x,0) \end{aligned} \tag{23}$$

By rearranging and substituting Eqs. (14) to 22 into Eq. (23), the following expression is derived:

$$\begin{aligned} &\frac{c^{init}_{NZ,w}}{1 + r\theta_{eq}\theta_{N^+}} - \frac{c^{init}_{NZ,w}}{1 + r(\theta_{eq}\theta_{Z^-})^{-1}} + \\ &\frac{c^{init}_{KA,w}}{1 + r\theta_{eq}\theta_{K^+}} - \frac{c^{init}_{KA,w}}{1 + r(\theta_{eq}\theta_{A^-})^{-1}} + \\ &\frac{c^{init}_{MX,w}}{1 + r\theta_{eq}\theta_{M^+}} - \frac{c^{init}_{MX,w}}{1 + r(\theta_{eq}\theta_{X^-})^{-1}} + \\ &\frac{rc^{init}_{OY,w}}{1 + r\theta_{eq}\theta_{O^+}} - \frac{rc^{init}_{OY,o}}{1 + r(\theta_{eq}\theta_{Y^-})^{-1}} = 0 \end{aligned} \tag{24}$$

This equation can be solved using the modified Powell hybrid method [62–64], obtaining $\Delta\phi_{eq}$ and with it the initial ion concentrations.

Additionally, the initial potential difference at the S|L interface must be defined at the beginning of the voltammogram. It can be calculated from the following Nernst equation:

$$\Delta_o^s\phi(0) = \Delta_o^s\phi_{Red}^{\circ} + \frac{RT}{F}\ln\left(\frac{c_{Ox^+}(0,t)}{c_{Red}(0,t)}\right) \quad (25)$$

As mentioned in Section 2, the ratio $\frac{c_{Ox^+}(0,t)}{c_{Red}(0,t)}$ was fixed at 10^{-6}. This yields $\Delta_o^s\phi(0) = \Delta_o^s\phi_{Red}^{\circ} - 0.355$ V.

Once these values are determined, the initial potential at equilibrium can be calculated as $E(0) = \Delta_o^s\phi(0) + [-\Delta_o^w\phi(0)]$, as shown in section 2.

References

[1] J. Koryta, M. Brezina, A. Hofmanová, D. Homolka, L.Q. Hung, M.W. Khalil, V. Mareček, Z. Samec, S. Sen, P. Vanýsek, Bioelectrochem. Bioenerg. 7 (1980) 61–68.
[2] Z. Samec, T. Kakiuchi, 4, VCH: Weinheim, Germany, 1995.
[3] A.G. Volkov, D.W. Deamer, D.L. Tanelian, John Wiley & Sons, New York, 1998.
[4] Y. Shao, Elsevier B.V., Oxford, 2007.
[5] R. Iglesias, S. Dassie, 129, Nova Publishers, New York, 2010.
[6] M. Senda, Y. Yamamoto, CRC Press, Boca Raton, Florida, 1996.
[7] A.N. Papov, Springer-Verlag. 1987.
[8] V.J. Cunnane, L. Murtomäki, CRC Press, Boca Raton, Florida, 1996.
[9] Z. Samec, Pure Appl. Chem. 76 (2004) 2147–2180.
[10] P. Peljo, H.H. Girault, Enc. Anal. Chem. (2012) 1–28.
[11] L.J. Sanchez Vallejo, J.M. Ovejero, R. Fernández, S. Dassie, Int. J. Electrochem. (2012) 34.
[12] Z. Samec, V. Mareček, J. Weber, J. Electroanal. Chem. Interfacial Electrochem. 100 (1979) 841–852.
[13] F. Marken, R.D. Webster, S.D. Bull, S.G. Davies, J. Electroanal. Chem. 437 (1997) 209–218.
[14] F. Scholz, Š. Komorsky-Lovrić, M. Lovrić, Electrochem. Commun. 2 (2000) 112–118.
[15] V. Mirčeski, R. Gulaboski, F. Scholz, Electrochem. Commun. 4 (2002) 814–819.
[16] M. Donten, Z. Stojek, F. Scholz, Electrochem. Commun. 4 (4) (2002) 324–329.
[17] G. Bouchard, A. Galland, P.-A. Carrupt, R. Gulaboski, V. Mirčeski, F. Scholz, H. Girault, Phys. Chem. Chem. Phys. 5 (17) (2003) 3748–3751.
[18] R. Gulaboski, A. Galland, K. Caban, A. Kretschmer, P.-A. Carrupt, Z. Stojek, H. Girault, F. Scholz, J. Phys. Chem. B 108 (14) (2004) 4565–4572.
[19] Š. Komorsky-Lovrić, V. Mirčeski, C. Kabbe, F. Scholz, J. Electroanal. Chem. 566 (2) (2004) 371–377.
[20] F. Quentel, V. Mirčeski, C. Elleouet, M. L'Her, J. Phys. Chem. C 112 (39) (2008) 15553–15561.
[21] H. Deng, X. Huang, L. Wang, Langmuir 26 (24) (2010) 19209–19216.
[22] K. Hu, B. Xu, H. Shao, Electrochem. Commun. 50 (2015) 36–38.
[23] C. Shi, F.C. Anson, Anal. Chem. 70 (15) (1998) 3114–3118.
[24] C. Shi, F.C. Anson, J. Phys. Chem. B 102 (49) (1998) 9850–9854.
[25] H.O. Shafer, T.L. Derback, C.a. Koval, J. Phys. Chem. B 104 (5) (2000) 1025–1032.
[26] F. Quentel, V. Mirčeski, M. L'Her, Anal. Chem. 77 (7) (2005) 1940–1949.
[27] R. Gulaboski, V. Mirčeski, C.M. Pereira, M.N.D.S. Cordeiro, A. Silva, F. Quentel, M. L'Her, M. Lovrić, Langmuir 22 (7) (2006) 3404–3412.
[28] M. Zhou, S. Gan, L. Zhong, B. Su, L. Niu, Anal. Chem. 82 (18) (2010) 7857–7860.
[29] L. Zhong, M. Zhou, S. Gan, Y. Bao, X. Dong, L. Niu, L. Guo, Electrochem. Commun. 13 (3) (2011) 221–224.
[30] S. Gan, M. Zhou, J. Zhang, L. Zhong, J. Ulstrup, L. Niu, Electroanalysis 25 (4) (2013) 857–866.
[31] V. Mirceski, B. Mitrova, V. Ivanovski, N. Mitreska, A. Aleksovska, R. Gulaboski, J. Solid State Electrochem. 19 (8) (2015) 2331–2342.
[32] J. Gu, W. Zhao, Y. Chen, X. Zhang, X. Xie, S. Liu, X. Wu, Z. Zhu, M. Li, Y. Shao, Anal. Chem. 87 (23) (2015) 11819–11825.
[33] C.E. Banks, T.J. Davies, R.G. Evans, G. Hignett, A.J. Wain, N.S. Lawrence, J.D. Wadhawan, F. Marken, R.G. Compton, Phys. Chem. Chem. Phys. 5 (19) (2003) 4053–4069.
[34] M. Opallo, A. Lesniewski, J. Niedziolka, E. Rozniecka, G. Shul, Rev. Polarography 54 (1) (2008) 21–30.
[35] F. Scholz, Annu. Rep. Prog. Chem., Sect. C: Phys. Chem. 102 (2006) 43–70.
[36] D. Kaluza, W. Adamiak, M. Opallo, M. Jonsson-Niedziolka, Electrochim. Acta 132 (2014) 158–164.
[37] F. Scholz, U. Schröder, R. Gulaboski, A. Doménech-Carbó, second ed., Springer, New York, 2015.
[38] T. Kakiuchi, Anal. Chem. 68 (20) (1996) 3658–3664.
[39] Q. Fulian, J.C. Ball, F. Marken, R.G. Compton, A.C. Fisher, Electroanalysis 12 (13) (2000) 1012–1016.
[40] Š. Komorsky-Lovrić, M. Lovrić, F. Scholz, Collect. Czechoslov. Chem. Commun. 66 (3) (2001) 434–444.
[41] Š. Komorsky-Lovrić, M. Lovrić, F. Scholz, J. Electroanal. Chem. 508 (1-2) (2001) 129–137.
[42] J.C. Myland, K.B. Oldham, J. Electroanal. Chem. 530 (1-2) (2002) 1–9.
[43] M. Lovrić, F. Scholz, J. Electroanal. Chem. 540 (2003) 89–96.
[44] V. Mirčeski, R. Gulaboski, F. Scholz, J. Electroanal. Chem. 566 (2) (2004) 351–360.
[45] V. Mirčeski, F. Quentel, M. L'Her, A. Pondaven, Electrochem. Commun. 7 (11) (2005) 1122–1128.
[46] Š. Komorsky-Lovrić, M. Lovrić, Open Chem. 3 (2) (2005) 216–229.
[47] M. Lovrić, Š. Komorsky-Lovrić, J. Solid State Electrochem. 10 (10) (2006) 852–856.
[48] Š. Komorsky-Lovrić, M. Lovrić, ChemElectroChem 1 (2) (2014) 436–440.
[49] M. Zhou, S. Gan, L. Zhong, X. Dong, J. Ulstrup, D. Han, L. Niu, Phys. Chem. Chem. Phys. 14 (10) (2012) 3659.
[50] M. Opallo, A. Lesniewski, J. Electroanal. Chem. 656 (1) (2011) 2–16.
[51] J. Koryta, Electrochim. Acta 32 (3) (1987) 419–424.
[52] Z. Samec, A. Trojánek, J. Langmaier, E. Samcová, J. Electroanal. Chem. 481 (1) (2000) 1–6.
[53] A. Molina, C. Serna, J. Gonzalez, J.A. Ortu no, E. Torralba, Phys. Chem. Chem. Phys. 11 (8) (2009) 1159–1166.
[54] A. Molina, C. Serna, J.A. Ortuno, E. Torralba, Annu. Rep. Prog. Chem., Sect. C: Phys. Chem. 108 (1) (2012) 126–176.
[55] P. Beattie, R. Wellington, H. Girault, J. Electroanal. Chem. 396 (1) (1995) 317–323.
[56] T. Kakiuchi, M. Senda, J. Electroanal. Chem. Interfacial Electrochem. 300 (1-2) (1991) 431–445.
[57] R. Iglesias, S. Dassie, A. Baruzzi, J. Electroanal. Chem. 556 (2003) 23–33.
[58] D. Britz, Lecture Notes in Physics, 666, Springer Berlin Heidelberg, Berlin, Heidelberg, 2005, 153.
[59] J. Garcia, R. Iglesias, S. Dassie, J. Electroanal. Chem. 580 (2) (2005) 255–264.
[60] J.I. Garcia, M.B. Oviedo, S.A. Dassie, J. Electroanal. Chem. 645 (1) (2010) 1–9.
[61] F. Scholz, U. Schröder, R. Gulaboski, 2005.
[62] E. Ziegel, W. Press, B. Flannery, S. Teukolsky, W. Vetterling, 29 (1987) 501.
[63] R.L. Burden, J.D. Douglas Faires, Análisis Numérico, México, 1985.
[64] http://www.netlib.org, 2016.
[65] N. Laanait, J. Yoon, B. Hou, P. Vanysek, M. Meron, B. Lin, G. Luo, I. Benjamin, M.L. Schlossman, J. Chem. Phys. 132 (17) (2010) 171101.
[66] A.J. Olaya, M.A. Méndez, F. Cortes-Salazar, H.H. Girault, J. Electroanal. Chem. 644 (1) (2010) 60–66.
[67] http://sbsrv7.epfl.ch/instituts/ isic/lepa/cgi/DB/InterrDB.pl, 2016.
[68] L.Q. Hung, J. Electroanal. Chem. Interfacial Electrochem. 115 (1980) 159–174.
[69] L. Hung, J. Electroanal. Chem. Interfacial Electrochem. 149 (1983) 1–14.
[70] S.A. Dassie, J. Electroanal. Chem. 728 (728) (2014) 51–59.
[71] P. Peljo, M. Bichon, H.H. Girault, Chem. Commun. 52 (2016) 9761–9764.
[72] J. Garcia, R. Fernández, S. Dassie, T. Kakiuchi, J. Electroanal. Chem. 640 (1) (2010) 42–50.